

Trellis Coded MPSK Modulation Techniques for MSAT-X¹

Dr. Dariush Divsalar and Dr. Marvin K. Simon
Mobile Satellite Program, Jet Propulsion Laboratory
California Institute of Technology, United States of America

Jet Propulsion Laboratory
4800 Oak Grove Drive 238-420
Pasadena, California 91109
United States of America

Abstract

This paper considers various trellis coded MPSK modulation techniques for transmitting 4.8 kbps over a 5 kHz RF channel. The tradeoffs between coherent versus differentially coherent types of demodulation, and interleaving versus no interleaving will be addressed. Optimum trellis codes which have been designed for fading channels will be discussed. These coding and modulation techniques have been proposed for NASA's MSAT-X project. Simulation results are presented. The paper also discusses many issues that should be considered in designing trellis coded modulation systems for fading channels.

Introduction

Transmission of 4800 bps in a power and bandwidth limited 5 kHz land mobile satellite channel is a formidable goal especially given a required bit error rate (BER) performance of 10^{-3} at an average bit signal-to-noise ratio (SNR) of 10-11 dB to ensure good quality digital speech. Analysis of these link requirements reveals that multilevel signaling with trellis coding is essential which, of course, is functionally more complex than the simpler uncoded formats. It has been concluded that a 10 dB SNR figure is required for UHF operation. For operation in L-band, this figure has been increased to 11 dB to cope with an almost doubling in Doppler effects due to the change in carrier frequency.

The work described herein focuses on the performance of two modulation and detection techniques based on octa-phase-shift-keying (8PSK) with trellis encoding and symbol interleaving for the UHF and L-band channel models described below (also see [1,2]). The techniques are referred to as the Dual Tone Calibrated Technique (DTCT) and differentially encoded 8-PSK (8DPSK) with differential detection and Doppler correction [3]. The 8DPSK system has been shown to have the better performance of the two under the assumed operating conditions; consequently, it will be described in greater detail.

Land Mobile Satellite Fading Channel Model

One of the important considerations in the development of the modem is the effect of propagation on the modulation and coding scheme. In this section, we briefly describe the Rician fading model which is characteristic of the land mobile satellite channel. Based on

¹This work was performed at the Jet Propulsion Laboratory, California Institute of Technology, under a contract with the National Aeronautics and Space Administration.

this model, a software program was written to simulate the fading channel [4].

An RF signal at 1.5 GHz with circular polarization transmitted by a satellite to a moving vehicle in a typical land environment exhibits extreme variation in both amplitude and apparent frequency. Fading effects are due to the random distribution of the electromagnetic field in space and originate from the motion of the vehicle. Here the field is expressed by a linear superposition of plane waves of random phase with component plane waves associated with the Doppler shift. This shift is due to the vehicle motion and is a function of mobile velocity, carrier frequency, and the angle that the propagation vector makes with the velocity vector. The power spectrum of the received signal depends on the density of the arrival angles of the plane waves and the mobile antenna directivity pattern. The instantaneous frequency of the signal received at the mobile has a random variation.

We can identify three components in the received faded signal at the mobile antenna, namely, the direct line of sight (LOS) component, the specular component, and the diffuse component. These correspond to the channel model illustrated in Figure 1. The combined direct and specular components are usually referred to as the *coherent* received component and the diffuse component is referred to as the *noncoherent* received component. In this model, it is assumed that only the coherent component can be attenuated by a lognormal distributed shadowing process due to the presence of trees, poles, buildings, and vegetation in the terrain. If the received coherent component is totally blocked, then the noncoherent component dominates and the received signal envelope variation has a Rayleigh distribution.

As shown by propagation studies [5], a typical land mobile satellite channel has a strong direct component in the presence of fading; thus the resulting received signal has a Rician distribution. For the present application, the Rician fade factor, K , i.e., the ratio of the coherent signal component power to the noncoherent signal component power is assumed to be 10 dB.

The one-way Doppler frequency shift due to vehicle motion can be computed from $f_d = (v/c)f_c$ where v is the mobile velocity, c is the speed of light, and f_c is the carrier frequency. The maximum value of f_d is assumed to be 100 Hz for UHF and 200 Hz for L-band corresponding to a mobile speed of 80 mph.

A complex representation of the fading channel mathematical model used to assess the performance of trellis coded modulation (TCM) systems is illustrated in Figure 2. In the figure, $F(t)$ represents the fading process, $m(t)$ represents the lognormal shadowing process, $N(t)$ is a complex Gaussian noise process, and $\omega_d = 2\pi f_d$. Simulation of this fading channel model indicates that at a fade depth of -3 dB and a Doppler spread of 40 Hz at L-band, the average duration of a fade is 20 symbols with a standard deviation of 10 symbols. Knowledge of the fade duration statistics enables us to design the correct interleaver structure for the TCM schemes.

The 16-State Trellis Coded 8DPSK System

A 16-state trellis coded 8DPSK system has been proposed for the NASA's MSAT-X project for operation at L-band [2,3]. A block diagram of the system is illustrated in Figure 3. Input bits at 4800 bps are passed through a rate 2/3, 16-state trellis encoder [6]. This encoder has been chosen because of its low complexity and good Euclidean distance ($d_{free}^2 = 5.17$). More important, however, is the fact that this code provides a "diversity" of three which makes it particularly attractive for the fading channel application. The meaning of "diversity" as used here will be

explained shortly in the section on design criteria.

The encoder output symbols are then block interleaved to break up burst errors caused by amplitude fades of duration greater than one symbol time. The block interleaver can be regarded as a buffer with d rows representing the *depth* of interleaving and s columns represent the *span* of interleaving. Data is written into the buffer in successive rows and read out of the buffer in successive columns. At the receiver, the block deinterleaver performs the reverse operation.

The interleaving depth should be chosen on the order of the average plus three times the standard deviation of the burst fade duration at a given fade depth related to the operating point. With this definition, at a fade depth of -3 dB for example, the fade duration at 40 Hz Doppler spread (15 mph) is on the order of 50 symbols (note that the fade duration is longer at low vehicle speeds).

The interleaving span should be chosen on the order of the decoder buffer size. Due to a delay constraint imposed by the requirement to transmit speech, the size (product of the depth and the span) of the block interleaver and deinterleaver has been chosen equal to 128 8-PSK symbols. For this size, the interleaving depth was optimized by computer simulation and found to be equal to 16 symbols. Thus, the interleaving span was chosen as 8 symbols. As noted above, at low speeds, e.g., 15 mph, an interleaving depth of 50 symbols is required which is greater than the 16 symbol depth chosen for the design. Thus, the 128 symbol interleaver size is really not sufficient and one should anticipate some performance penalty because of this limitation.

The interleaved trellis-encoded symbols are next differentially encoded and pulse-shaped using root raised cosine filters with 100% excess bandwidth. This pulse shaping is used to limit adjacent channel interference to an acceptable value. The output of the pulse-shaping filters modulates quadrature RF carriers for transmission over the fading channel.

At the receiver, the faded, noise-corrupted signal is downconverted by sampling, and then passed through brick wall filters with bandwidth equal to the sum of the 8-PSK symbol rate plus the maximum Doppler shift, i.e., $2400 \text{ sps} + 200 \text{ Hz} = 2600 \text{ Hz}$. The outputs of the brick wall filters are provided to the Doppler frequency estimator and to pseudo-matched filters (consisting of a brick wall filter and a half symbol delay and add circuit). In the absence of Doppler frequency shift, these pseudo-matched filters are exactly root raised cosine filters [7]. Details of the operation and performance of the Doppler estimator can be found in [3]. An illustration of its performance (rms Doppler error versus bit SNR) over the AWGN and the fading channel is shown in Figure 4 for 8DPSK. The parameter K_{α} represents the effective number of symbols of integration [3] for the LPF in the Doppler Estimator of Figure 3. The outputs of the pseudo-matched filters are provided to a differential detector and then to a residual Doppler correction circuit. The differentially detected and Doppler corrected samples are then fed to the deinterleaver and finally to the trellis decoder. At the trellis decoder, branch metrics are computed using a correlation (Gaussian noise) metric. It can be shown that, in the absence of channel state information (CSI), this metric is approximately optimum. Each symbol time, branch metrics are provided to the Viterbi algorithm which consists of add-compare-select operations with state metric normalization to prevent buffer overflow. The size of the survivor path's buffer is chosen to be 32 symbols based on computer simulation tests. These tests have also shown that the difference in performance between a 32 symbol buffer and a 256 symbol buffer is on the order of a few tenths of a dB.

A software simulation program has been written for the system shown in Figure 3. In the simulation, floating point operation has been used and perfect timing and perfect Doppler

estimation have been assumed. Results of this simulation [3] show that with the appropriate choice of digital filter bandwidth in the Doppler estimator, there will be about 0.5 dB degradation due to the Doppler estimation error. Other simulation results for end-to-end bit error probability of the system of Figure 3 are illustrated in Figures 5 and 6.

This system has been implemented at JPL [8] using TMS32020 DSP chips. The measured bit error probabilities agree with the simulation results given here within 1 dB.

The 16-State Trellis Coded 8PSK System with Pilot-Aided Coherent Detection

This system was proposed in [1] for NASA's MSAT-X project to be used at UHF. A block diagram of the system is illustrated in Figure 7. Most components of this system are identical to those in Figure 3. The differences between the two are as follows. For coherent detection, we use two pilot tones which are inserted at the edges of the signal spectrum as shown on the figure. At the receiver, the faded, noise-corrupted signal is demodulated with pilot tones derived from the pilot tone extraction unit [9, 10] also illustrated in the figure. Unfortunately, this coherent demodulation technique introduces a 180° phase ambiguity. To resolve this ambiguity, the input bits to the trellis encoder should be differentially encoded and the output bits of the trellis decoder should be differentially decoded. Furthermore, the trellis code must be transparent to a 180° phase shift. Unfortunately, the rate $2/3$, 16-state Ungerboeck code [6] does not have this transparency property.

We have designed a rate $2/3$, 16-state trellis code (Figure 8) with a diversity [11] of three that is transparent to a 180° phase shift but is slightly inferior (approximately less than 0.2 dB for all error probabilities greater than 10^{-6}) to the above Ungerboeck code. Simulation results for this new code are illustrated in Figure 9.

Design Criterion

It has been shown [11], that the appropriate criterion for designing trellis codes for the fading channel is to maximize the minimum of the squared distance

$$d^2 = \sum_{\eta \in \eta} \frac{\alpha K \delta_n^2}{1 + K + \beta \delta_n^2} + \left(\frac{E_s}{4N_0} \right)^{-1} \ln \frac{1 + K + \beta \delta_n^2}{1 + K} \quad (1)$$

computed over all possible error events in the trellis diagram. Here δ_n^2 represents the squared Euclidean distance between the n th transmitted (correct) and estimated (incorrect) symbols along an error event path and η is the set of possible occurrences of such errors along that path. Also, for coherent detection with ideal channel state information (CSI)

$$\alpha = 1, \quad \beta = \frac{\bar{E}_s}{4N_0} \quad (2)$$

and for differentially coherent detection with no CSI

$$\alpha = \frac{1}{2}, \quad \beta = \frac{\bar{E}_s}{8N_0} - \frac{1 + K}{16} \quad (3)$$

where E_s/N_0 is the average received symbol SNR and K is again the Rician fade parameter.

Among the class of Ungerboeck codes [6] with low complexity, the rate $2/3$, 16 state code seems to be very attractive. Indeed using our design criterion, it can be shown that the Ungerboeck code (multiplicity one) designed for the AWGN is also optimum on the fading channel and

achieves a diversity [11] of three.

Among the class of multiple trellis codes [12] investigated, the two state code with multiplicity two (see Figure 10) is very simple, effective, and optimum over Rayleigh channels. Note that this code is not optimum over the AWGN channel. The optimum code for the AWGN channel is illustrated in Figure 11 for comparison. Simulation results for these two rate 4/6 codes are illustrated in Figures 12 and 13.

References

- [1] D. Divsalar and M.K. Simon, "Trellis Coded Modulation for 4800 to 9600 bps Transmission Over a Fading Satellite Channel," JPL Pub. 86-8 (MSAT-X Report No. 129), June 1, 1986. Also see IEEE Journal on Selected Areas in Commun., Vol. SAC-5, No. 2, February 1987, pp. 162-175.
- [2] M. K. Simon, D. Divsalar, "The Performance of Trellis Coded Multilevel DPSK on a Fading Mobile Satellite Channel," JPL Pub. 87-8 (MSAT-X Report No. 144), Pasadena, CA, June 1, 1987. Also to appear in the February 1988 issue of the IEEE Transactions on Vehicular Technology.
- [3] M. K. Simon, D. Divsalar, "Doppler-Corrected Differential Detection of MPSK," accepted for publication in the IEEE Transactions on Communications.
- [4] D. Divsalar, "JPL's Mobile Communication Channel Software Simulator," Proceedings of the Propagation Workshop in Support of MSAT-X (JPL Internal Document D-2208), Jet Propulsion Laboratory, Pasadena, CA, January 30-31, 1985.
- [5] W.J. Vogel, "Land Mobile Radio Propagation Measurements at 869 and 1501 MHz," 1985 North American Radio Science Meeting, UBC, Vancouver (URSI Abstract Booklet), June 17-21, 1985, Paper N. F-2-1,, p. 348.
- [6] G. Ungerboeck, "Channel Coding with Multilevel/Phase Signals," IEEE Transactions on Information Theory, Vol. IT-28, No. 1, January 1982, pp. 55-67.
- [7] T. Jedrey, private communication.
- [8] N. Lay, T. Jedrey, D. Divsalar, C. Cheetham, D. Black, "Modem and Terminal Processor Testing on the JPL Fading Channel Simulator," MSAT-X Quarterly, No. 15, Jet Propulsion Laboratory, Pasadena, CA, April 1988.
- [9] W. Rafferty, et al., "A Proposed Design for a Land Mobile Satellite Terminal," a proposal submitted to JPL by the General Electric Co., Corp. R&D, New York, 1985.
- [10] M. K. Simon, "Dual Pilot Tone Calibration Technique (DPTCT)," IEEE Transactions on Vehicular Technology, Vol. VT-35, No. 2, May 1986, pp. 63-70.
- [11] D. Divsalar, M.K. Simon, "The Design of Trellis Codes for Fading Channels," JPL Pub. 87-39 (MSAT-X Report 147), Pasadena, CA, November 1, 1987. Also to appear (in two parts) in a future issue of the IEEE Transactions on Communications.
- [12] D. Divsalar, M. K. Simon, "Multiple Trellis Coded Modulation (MTCM)," JPL Pub. 86-44 (MSAT-X Report No. 141), Pasadena, CA, November 15, 1988. Also to appear in a future issue of the IEEE Transactions on Communications.

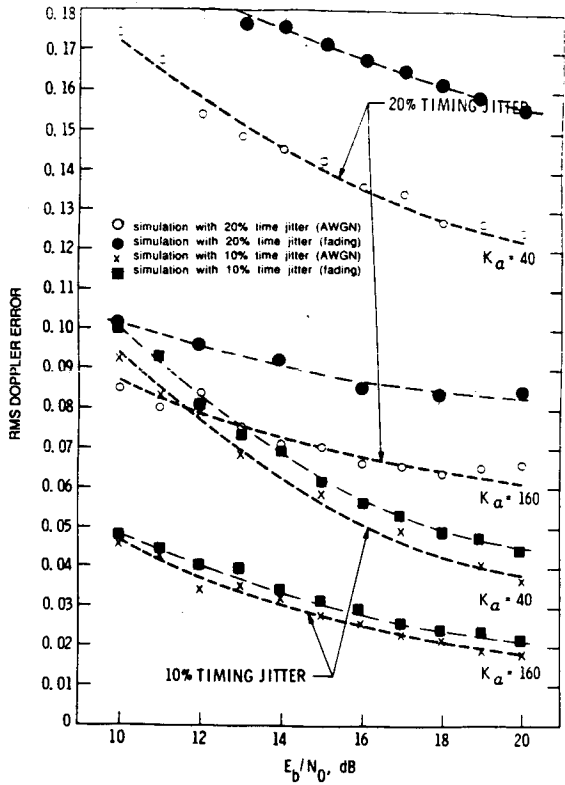


Figure 4. The RMS Doppler Error vs. the Bit Energy-To-Noise Ratio with 10% and 20% Time Jitter

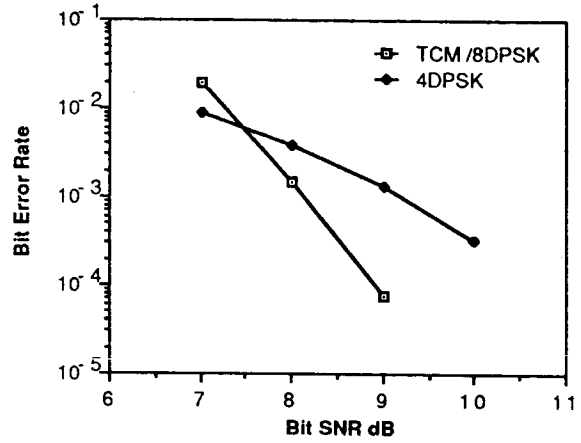


Figure 5. Simulation Results for the Bit Error Rate of Trellis Coded 8 DPSK and Uncoded 4 DPSK over AWGN Channel

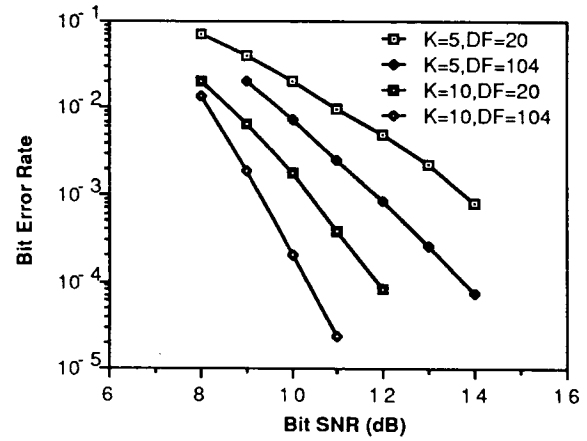


Figure 6. Simulation Results for the Bit Error Rate of Trellis Coded 8 DPSK over Rician Fading Channel with Rician Factor of 5dB, 10dB and Doppler Spread of 20Hz, 104 Hz

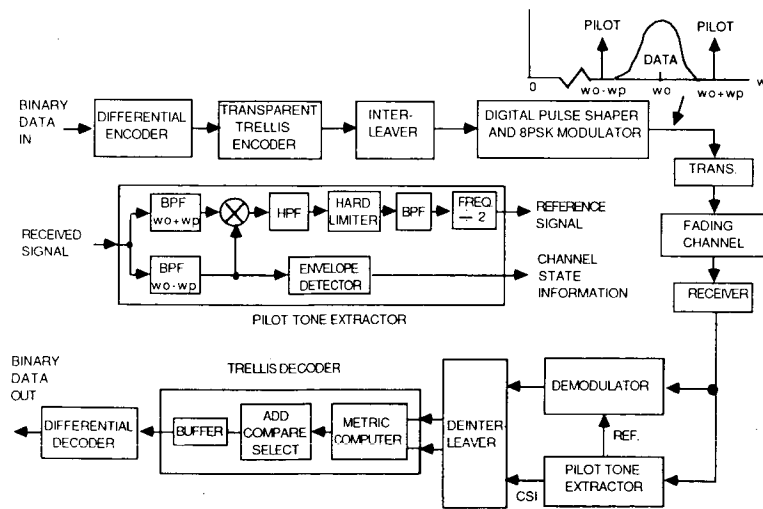


Figure 7. Block Diagram of Trellis Coded 8 PSK System with Pilot-Aided Coherent Detection

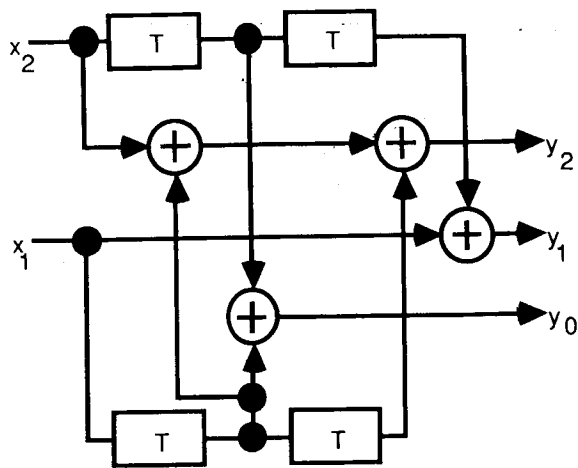


Figure 8. A New 180° Phase Invariant (Transparent) Trellis Encoder

RICIAN PARAMETER K = 10 dB PILOT BANDWIDTH = 200 Hz (UHF)
 DOPPLER SPREAD = 20 Hz (UHF) TOTAL POWER OF PILOTS/DATA POWERS = -7 dB (UHF)

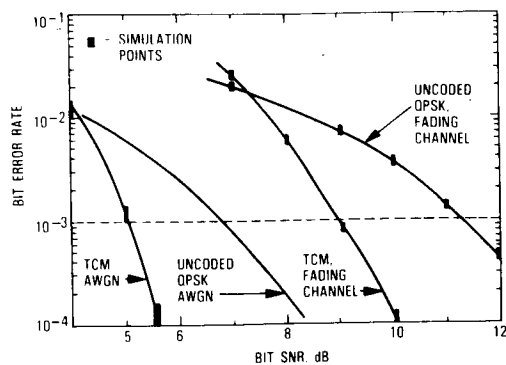


Figure 9. Simulation Results for the Bit Error Rate of Differentially Encoded, (Transparent) Trellis Coded 8 PSK with Pilot-Aided Coherent Detection

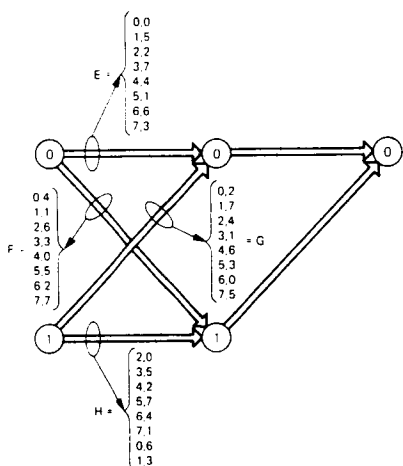


Figure 10. Trellis Diagram for Multiple (k=2), Rate 4/6 Coded 8 PSK; 2 States, Designed for Fading Channel

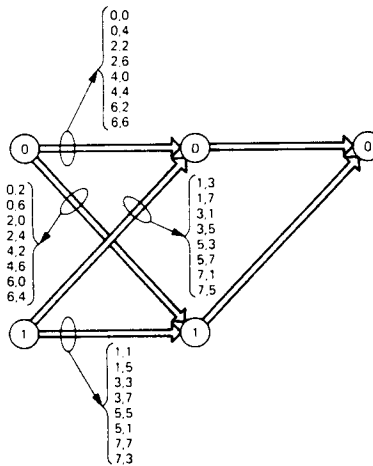


Figure 11. Trellis Diagram for Multiple (k=2), Rate 4/6 Coded 8 PSK; 2 States, Designed for a AWGN Channel

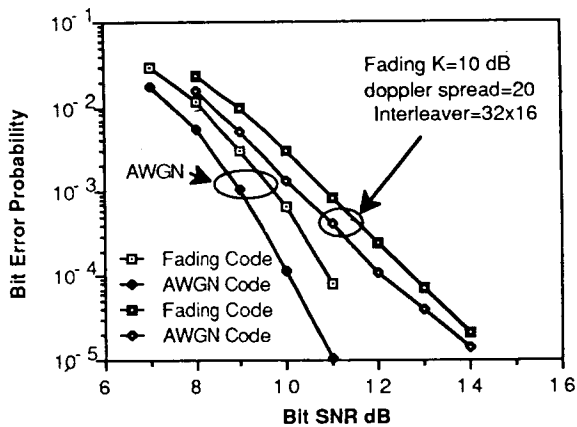


Figure 12. Simulation Results for Multiple Trellis Codes of Figures 10 and 11 with 8 DPSK over AWGN and Rician Fading (K=10dB) Channels

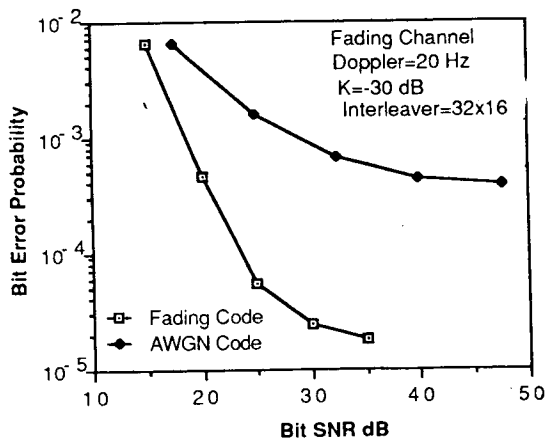


Figure 13. Simulation Results for Multiple Trellis Codes of Figures 10 and 11 with 8 DPSK over Rayleigh Fading Channel (K=30dB)